ChemComm

Rapid construction of fluorescence quenching-based immunosensor Q-bodies using α-helical coiled-coil peptides

Journal:	*ChemComm*
Manuscript ID	CC-COM-05-2021-002605.R1
Article Type:	Communication

COMMUNICATION

Rapid construction of fluorescence quenching-based immunosensor Q-bodies using α-helical coiled-coil peptides

Takanobu Yasuda [a], Akihito Inoue [a], Tetsuya Kitaguchi [b], and Hiroshi Ueda [b*]

Received 00th January 202x,
Accepted 00th January 202x

DOI: 10.1039/x0xx00000x

Here, we report a rapid and efficient method to fabricate Quenchbodies (Q-bodies) that can detect targets with antigen-dependent fluorescence augmentation using a stable coiled-coil peptide pair, E4 and K4 (coiled Q-body, CQ-body). The CQ-body allowed antigen detection not only in buffer but also in 50% plasma. Furthermore, we describe FRET-type CQ-bodies using a dual-coloured K4 peptide, which allowed a more precise antigen quantification. Lastly, successful fabrication of nanobody-based CQ-body shows its applicability to a range of antibody fragments.

Immunoassays that take advantage of antigen-antibody reactions are critical in the analysis and monitoring of trace substances in various experimental fields, including disease diagnosis, food/environmental analysis, and biological research[1-3]. Radioimmunoassays (RIA) were the first immunoassays using radioisotopes, enabling the detection of trace biological substances, including proteins and peptide hormones, which are difficult to monitor with chemical or physical analytical methods[4]. The widely used enzyme-linked immunosorbent assay (ELISA) detects target molecules using an enzyme reaction instead of a radioisotope. However, ELISA requires multiple washing steps to remove background signals, which are time-consuming and occasionally cause measurement errors.

Quenchbodies (Q-bodies) are antibody-based novel immunoassay tools that do not require bound/free separation and can noncompetitively detect various types of antigens[5]. Typically, a fluorescent dye is attached to the N-terminal region of the antibody, and the dye is quenched by intrinsic tryptophan residues present in the antibody variable region through photoinduced electron transfer. After antigen binding, the fluorescent dye moves outside of the antibody, and its fluorescence is recovered as the electron transfer from the tryptophan residues decreases[6]. Q-bodies allow for rapid and sensitive detection of target molecules by simply mixing with the sample. Thus, this technology is suitable for *in situ* detection of many antigens of interest.

To date, the Cys-tag method is most frequently used to achieve site-specific labelling of fluorescence dyes to fabricate Q-bodies. The maleimide dye is labelled with a cysteine residue by Michael addition and is incorporated into the N-terminal tag attached to the variable region of the antibody fragments[7, 8]. This Cys-tag method was successfully utilized for the cost-effective preparation of Q-bodies, and they were applied not only in vitro but also in cellular assays. However, the Cys-tag may trigger misfolding of recombinant antibody fragments during expression in *E. coli.* Furthermore, the extensive purification step to remove excess dye after labelling reduces Q-bodies yield.

Yano et al.[9] reported a rapid method for noncovalent fluorescence labelling of cell surface receptors without affecting their function. Instead of cysteine labelling, they used artificial negatively-charged E_n $(EIAALEK)_n$ and positively-charged K_n $(KIAALKE)_n$ (n = 3 or 4) heterodimeric coiled-coil peptide pairs[9] initially developed by Litowski and Hodges[10, 11]. The coiled-coil peptide approach was used successfully to quickly label (<1 min) E3 tags attached to the N-terminus of the mouse-derived prostaglandin EP3β receptor by adding fluorescence-dye-labelled K4 (Kd = 6 nM) to the culture media. This work showed that E and K coiled-coil peptides are useful for rapid fluorescence labelling of proteins with high affinity.

Here, we report the successful fabrication of a coiled Q-body (CQ-body) using a coiled-coil peptide pair comprised of E4 and K4. The CQ-body was formed by mixing a Fab fragment appended with an E4 peptide at the N-terminus with fluorescence labelled K4 for 10 min. We also used a dual-coloured K4 to successfully fabricate a Förster resonance energy transfer (FRET)-based CQ-body capable of more accurate antigen detection upon probe concentration changes. Furthermore, it was demonstrated that not only Fab fragment

[a] *Graduate School of Life Science and Technology, Tokyo Institute of Technology, 4259 Nagatsuta-cho, Midori-ku, Yokohama 226-8503, Japan.*
[b] *Laboratory for Chemistry and Life Science, Institute of Innovative Research, Tokyo Institute of Technology, 4259 Nagatsuta-cho, Midori-ku, Yokohama, 226-8503 Japan.*
† Electronic Supplementary Information (ESI) available: See DOI: 10.1039/x0xx00000x

but also nanobody (V_{HH}) can be transformed to a CQ-body, suggesting that this method is useful for rapid fabrication of Q-bodies from various antibody fragments.

Firstly, we constructed a vector expressing recombinant Fab tagged at the N-terminus with E3, which forms a heterodimer with a C-terminally fluorescence-labelled K4 peptide. An E4 sequence was also tested instead of E3 in a coiled-coil pair with K4 because of its higher affinity (estimated 14 pM)[10, 12]. Strep II tags for affinity purification were incorporated into Fab at the C-terminus of both the heavy chain (HC) and the light chain (LC). His tag was also incorporated into the C-terminus of HC for tandem purification (Figure 1A). The sequence of the anti-human osteocalcin (Bone Gla Protein, BGP) Fab fragment KTM219[13] was introduced into the vector to compare the antigen response of previously reported anti-BGP Fab-type Q-bodies[7, 14]. E3-Fab and E4-Fab were expressed in the cytosol of *E. coli* and purified using the Strep II and His tag. SDS-PAGE analysis revealed two clear bands corresponding to HC conjugated with E peptides and LC (upper and lower bands, respectively) (Figure 1B). We performed ELISA tests to confirm the antigen-binding activity of the recombinant Fabs. The wells immobilised with antigen had a significant absorbance signal compared to the wells without antigen (Figure 1C). These results indicate that each Fab retains sufficient antigen-binding activity, despite the presence of the E3 or E4 sequences at the N-terminus of HC.

We synthesised a C-terminally tetramethylrhodamine (TAMRA)-labelled K4 peptide (K4-T) and purified it by reverse-phase high-performance liquid chromatography (RP-HPLC). TAMRA is frequently used for constructing Q-bodies because its high quenching efficiency promotes the production of desired Q-bodies, with good fluorescence responses[5]. We then identified K4-T using MALDI-TOF/MS.

We measured the fluorescence intensity of the E3- or E4-Fab and K4-T mixtures in the presence of BGP-C7 antigen (C-terminal epitope peptide of BGP) to confirm the function of the CQ-body as an immunosensor. The tagged Fabs and TAMRA-labelled K4 were mixed at 1 µM and less than 1 µM, respectively, and incubated for 10 min to completely form heterodimers. We then measured the fluorescence intensity of 5 nM of the mixture before and after adding 1 µM of BGP-C7 antigen (Figure 2A). The fluorescence intensity was measured simultaneously in denaturant guanidium hydrochloride (Gdn-HCl), which produces the maximum dequenched status. As the result, the E4-CQ-body had a 2.4-fold increase in fluorescence upon antigen addition and a 2.7-fold response under denaturing conditions (Figure 2B). The antigen and denaturation conditions had similar effects on fluorescence intensity, indicating that TAMARA is quenched by Fab in its native state and almost completely dequenched upon antigen addition. Conversely, the E3-CQ-body did not significantly increase fluorescence intensity with antigen presence or denaturation, probably reflecting lower affinity of E3 to K4-T. To compare the quenching efficiency of E3- or E4-Fab towards K4-T, fluorescence titrations were performed. As a result, Fab-dependent fluorescence quenching was only observed for E4-Fab (up to 62.4%) but not for E3-Fab (Figure S1). Also, when the binding ability of E3- or

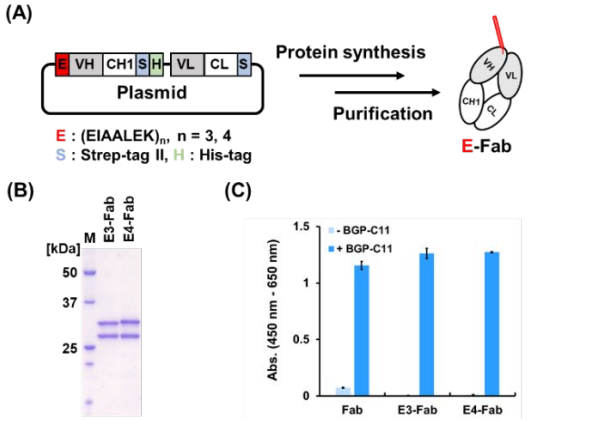

Fig. 1. (A) Scheme of the expression vector for anti-BGP Fab fragment with the E peptide sequence at the N-terminus of the heavy chain. **(B)** Coomassie brilliant blue stained image of SDS-PAGE analysis of the purified E3-Fab and E4-Fab. M: Precision Plus protein unstained standards (Bio-Rad); **(C)** Specific binding of the native and tagged Fab to antigens probed by ELISA. Average ± 1 SD of three samples is shown.

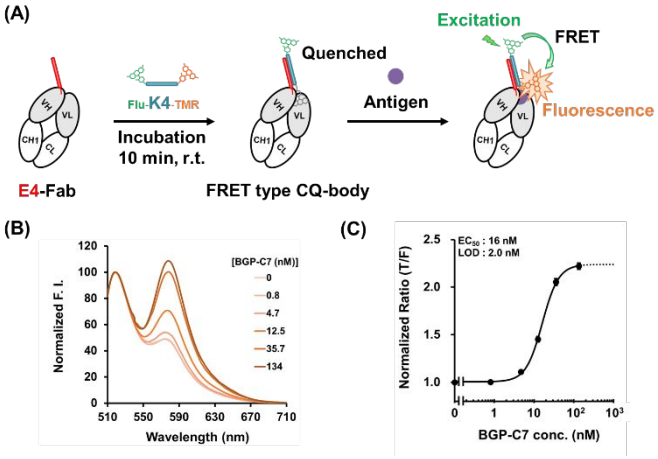

Fig. 2. (A) Schematic representation of the process for constructing a CQ-body using coiled-coil peptide conjugated E peptide and TAMRA labelled K4. **(B)** Fluorescence intensities of 5 nM CQ-bodies in the presence of 1 µM BGP-C7 or under denaturing condition. **(C)** Fluorescence spectra of 5 nM E4-CQ-body with excitation at 545 nm in the absence and presence of BGP-C7.

E4-Fab to K4 peptide was compared by ELISA, higher signal of E4-Fab than E3-Fab (Figure S2). From these results, we considered that E3-Fab was not suitable for use in a CQ-body due to its weaker affinity and the possibility of annealing at the undesired position far from the H chain N-terminus. Hence, we used E4-Fab for subsequent experiments. To further evaluate the binding specificity of the CQ-body, we performed the same assay with BGP-C10dV, which lacks the C-terminal valine, an essential epitope of this antibody[13]. No apparent increase in fluorescence was observed in the presence of BGP-C10dV (Figure S3). This suggests that the binding specificity of Fab for BGP is preserved, even in the presence of the N-terminal coiled-coil sequence. We measured the CQ-body fluorescence spectrum in the presence of the antigen and observed a dose-dependent increase up to 3.0-fold after BGP-C7 addition (Figure 2C). We infer that CQ-bodies with higher fluorescence response could be achieved by optimizing the linker length between E4

and Fab or K4 and TAMRA because the anti-BGP Fab Q-body produced by the Cys-tag method had a fluorescence response up to 7-fold[7]. The fluorescence intensity titration curve at the maximum point suggested that the fluorescence increased with BGP-C7 peptide concentration (Figure S4). By the curve fitting, the EC_{50} and limit of detection (LOD) were estimated as 17 nM and 5.6 nM, respectively. The EC_{50} value agreed with what was previously reported[7, 14]. To further demonstrate the utility of the CQ-body in clinical setting, we investigated its performance in 50% human plasma. The results showed that the fluorescence intensity increased with BGP-C7 concentration and that the antigen could be detected in the clinical sample (Figure S5).

We also investigated CQ-body stability and observed that it was possible to accurately detect an antigen at least until 3 h after preparation; this time period was sufficient to complete a Q-body assay. We performed time-course measurements with CQ-bodies incubated at 20 °C for 24 h after mixing E4-Fab and K4-T. The fluorescence intensity of CQ-bodies that were left in the incubator for 0–5 h in the absence of BGP-C7 was almost unchanged but more or less increased after 24 h (Figure S6A). The dose-response curves showed similar assay sensitivity at '0 h', '1 h', and '3 h', but there was a larger error on the '5 h' curve due to an unknown reason. The '24 h' curve indicated a relatively low fluorescence response due to an increase in the background signal (Figure S6B, Table S3). These results suggest that long incubations triggered the dissociation of the coiled-coil pair, or partial denaturation/inactivation of E4-Fab.

To expand CQ-body functionality, we introduced fluorescein as a fluorescent donor at the N-terminus of K4-T (F-K4-T), which allows ratio measurement of antigen by FRET. F-K4-T was mixed with E4-Fab to prepare a FRET-type CQ-body, and the fluorescence spectrum was measured in the presence of the antigen (Figure 3A). The fluorescein fluorescence peak decreased, and the TAMRA fluorescence peak increased proportionally to antigen concentration (Figure 3B). While the increase of TAMRA fluorescence can be explained by dequenching, the decrease of donor peak reflects the increased FRET efficiency possibly due to the outbound move of the TAMRA dye from the inside of the antibody upon antigen binding. Previous work showed that antigen binding moves TAMRA modified to variable region from the inside to the outside of the antibody[3]. The dose-response curve of the fluorescence peak ratio increased up to 2.2-fold, depending on BGP-C7 concentration. Using curve fitting, the EC_{50} and LOD values were estimated as 16 nM and 2.0 nM, respectively (Figure 3C). The FRET CQ-body should accurately quantify an antigen by the change in the fluorescence peak ratio even when probe concentrations vary. To test this, we measured the fluorescence intensity of 5 nM and 10 nM FRET type CQ-bodies upon TAMRA and fluorescein excitation in the presence of the antigen. Fluorescence intensity at 10 nM CQ-body reached approximately double the value at 5 nM when TAMRA was excited, which was directly proportional to probe concentration (Figure S7A). However, when fluorescein was excited, the titration curves were similar for 10 nM and 5 nM CQ-bodies and the antigen was detected, regardless of probe concentration (Figure S7B). Furthermore, the FRET-type CQ-body

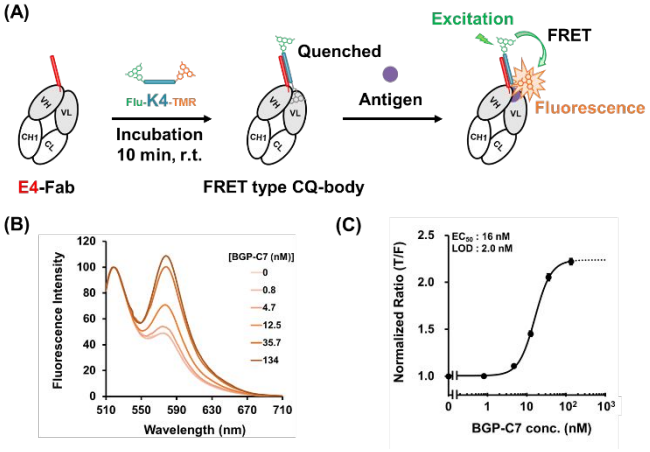

Fig. 3. (A) Schematic representation of the process for constructing a FRET type CQ-body using a coiled-coil peptide conjugated E4 and dual-coloured K4. Flu: Fluorescein; **(B)** Normalized fluorescence spectra of 5 nM FRET type CQ-body with excitation at 480 nm in absence and presence of BGP-C7. **(C)** Dose-response curve for BGP-C7. The top intensities of TAMRA were divided by those of fluorescein and then the normalized ratio was calculated and plotted.

quantitatively detected BGP-C7 even in the presence of 20% human serum excited at either 545 nm or 480 nm (Figure S8), suggesting the possible use of FRET CQ-body in clinical diagnostic applications.

To better understand the mechanism of antigen dependent FRET efficiency change, we investigated the change in the fluorescence ratio with K4 variants at different FITC and TAMRA distances on the peptide; K4-T at the N-terminus, Lys6, Lys13, and Lys20 were labelled with FITC (Figure S9). At first, to investigate the influence of FITC labelling of internal Lys in the K4, fluorescence titrations of 1 nM K4-T and K4(Lys13F)T with E4-Fab were performed. The result showed the EC_{50} of K4-T as 3.9 nM, while that of K4(Lys13F)T as 12 nM, indicating the importance of the positive charge of Lys13 in the K4 (Figure S10). However, due to the higher concentration of E4-Fab (1 μM) and K4-T (somewhat less than 1 μM) during the fabrication of CQ-body, we assumed that the effect of FITC labelling to Lys in K4 was negligible for the dimerization with E4-Fab. Next, dual-coloured K4 variants were used to generate CQ-bodies and fluorescence spectra measured with excitation at 480 nm. In overall, the decrease in fluorescence intensity was observed as the distance between the two dyes decreased (Figure S11). This was probably due to increased FRET efficiency between the two dyes, but additional quenching due to static dye-dye interaction might lead to deeper quenching[15]. Also, the fluorescence peak ratio (TAMRA/FITC) in the absence or presence of antigen increased as the distance between donor and acceptor decreased (Table S4), showing increased FRET efficiency. To perform more precise investigation, the irradiation-based and FRET-based dose-responses were determined using a microplate reader (Figure S12). It is worth nothing that the maximum FRET-based responses were consistently higher than its irradiation-based responses, probably reflecting increased FRET efficiency change (Table S5). In contrast, the antigen response decreased with both irradiation- and FRET-based CQ-body as fluorescein became closer to TAMRA. Therefore, we

expect that using a fluorescent protein or a luminescent enzyme as a donor that does not form dimer with TAMRA should create CQ-bodies with higher fluorescence or luminescence intensity in future.

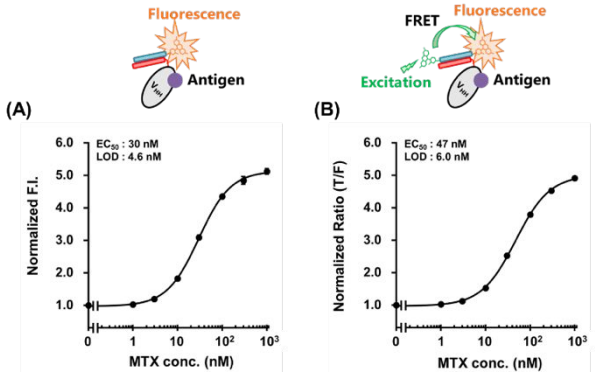

Fig. 4. Does-response of mini CQ-body **(A)** and FRET type mini CQ-body **(B)** for MTX. Protein concentration was 5 nM for each assay.

Finally, to explore the potential of E4 and K4 for fabricating CQ-body from various antibody fragments, nanobody (also called V_{HH})[16] was used. Nanobody is a single variable domain derived from the heavy-chain-only antibody in Camelidae, and it has characteristics such as its lower molecular weight and robustness to harsh conditions[17]. Anti-methotrexate (MTX) V_{HH} was incorporated E4 sequence into its N-terminus was prepared. Then, E4-V_{HH} was mixed with K4-T and measured its fluorescence intensity upon adding various concentration of MTX using a microplate reader as before. The dose-response curve increased up to 5.1-fold, depending on MTX concentration. Using curve fitting, the EC_{50} and LOD values were estimated as 30 nM and 4.6 nM, respectively (Figure 4A). The result was in good agreement with the previous result for anti-MTX Q-body (response : approximately 6.0-fold, EC_{50} : 37.6 nM, LOD : 0.56 nM)[18]. Moreover, FRET type mini CQ-body was also successfully made using F-K4-T (Figure 4B). These results suggest that many antibody fragments with different formats can be transformed into CQ-bodies.

In conclusion, we successfully converted anti-BGP Fab and anti-MTX V_{HH} fragments into Q-bodies within 10 min using a coiled-coil peptide pair, E4 and K4. This novel approach is simpler and faster than any previously proposed methods for generating Q-bodies. We expect that this method will also allow us rapid adjustment of linker length and the selection of fluorescent dyes by preparing a K4 library. We also successfully developed a FRET-type CQ-body capable of more accurately quantifying antigens by introducing another dye as a donor into K4-T. Because it was more resistant to probe concentration change, we expect this approach to be applied for various applications such as cellular imaging where the local probe concentration may significantly vary. Finally, this E4-K4 engineering will be applicable to many other protein-protein conjugation and protein labelling reactions. It does not need any steps for enzyme reaction or separation. We envisage this technology will advance not only Q-body technology but also many other bioconjugation technologies.

Conflicts of Interest

There are no conflicts to declare.

Acknowledgements

This work was supported in part by the JSPS KAKENHI Grant Number JP18H03851 (to H.U.) from the Japan Society for the Promotion of Science, Japan, and by the JST-Mirai Grant Number JPMJMI18D9 (to H.U.) from the Japan Science and Technology Agency, Japan. We thank Chiaki Toyama and Atsushi Izutani for experimental help, and the Division of Bio-material Analysis, Open Facility Center, Tokyo Institute of Technology, for nucleic acid sequence analysis.

Notes and references

1. J. Wang, C. Jiang, J. Jin, L. Huang, W. Yu, B. Su and J. Hu, *Angew. Chem. Int. Ed.*, 2021. doi: 10.1002/anie.202103458
2. Y. Kabe, S. Sakamoto, M. Hatakeyama, Y. Yamaguchi, M. Suematsu, M. Itonaga and H. Handa, *Anal. Bioanal. Chem.*, 2019, **411**, 1825-1837.
3. H. U. Rahman, X. F. Yue, Q. Y. Yu, H. L. Xie, W. Zhang, Q. Zhang and P. W. Li, *J. Sci. Food. Agric.*, 2019, **99**, 4869-4877.
4. R. S. Yalow and S. A. Berson, *J. Clin. Invest.*, 1960, **39**, 1157-1175.
5. R. Abe, H. Ohashi, I. Iijima, M. Ihara, H. Takagi, T. Hohsaka and H. Ueda, *J. Am. Chem. Soc.*, 2011, **133**, 17386-17394.
6. H. Ohashi, T. Matsumoto, H. Jeong, J. Dong, R. Abe and H. Ueda, *Bioconjug. Chem.*, 2016, **27**, 2248-2253.
7. R. Abe, H. Jeong, D. Arakawa, J. Dong, H. Ohashi, R. Kaigome, F. Saiki, K. Yamane, H. Takagi and H. Ueda, *Sci. Rep.*, 2014, **4**.
8. H. Jeong, T. Kawamura, J. Dong and H. Ueda, *ACS Sens.*, 2016, **1**, 88-94.
9. Y. Yano, A. Yano, S. Oishi, Y. Sugimoto, G. Tsujimoto, N. Fujii and K. Matsuzaki, *ACS Chem. Biol.*, 2008, **3**, 341-345.
10. J. R. Litowski and R. S. Hodges, *J. Biol. Chem.*, 2002, **277**, 37272-37279.
11. D. Lindhout, J. Litowski, P. Mercier, R. Hodges and B. Sykes, *Biopolymers*, 2004, **75**, 367-375.
12. K. Groger, G. Gavins and O. Seitz, *Angew. Chem. Int. Ed.*, 2017, **56**, 14217-14221.
13. S. L. Lim, H. Ichinose, T. Shinoda and H. Ueda, *Anal. Chem.*, 2007, **79**, 6193-6200.
14. J. Dong, H. Jeong and H. Ueda, *J. Biosci. Bioeng.*, 2016, **122**, 125-130.
15. A. Wei, D. Blumenthal and J. Herron, *Anal. Chem.*, 1994, **66**, 1500-1506.
16. C. Hamerscasterman, T. Atarhouch, S. Muyldermans, G. Robinson, C. Hamers, E. B. Songa, N. Bendahman and R. Hamers, *Nature*, 1993, **363**, 446-448.
17. R. H. J. van der Linden, L. G. J. Frenken, B. de Geus, M. M. Harmsen, R. C. Ruuls, W. Stok, L. de Ron, S. Wilson, P. Davis and C. T. Verrips, *Biochim. Biophys. Acta-Protein Struct. Mol. Enzymol.*, 1999, **1431**, 37-46.
18. A. Inoue, Y. Ohmuro-Matsuyama, T. Kitaguchi and H. Ueda, *ACS Sens.*, 2020, **5**, 3457-3464.